Journal of Solid State Chemistry 184 (2011) 1085–1089

Contents lists available at ScienceDirect

Journal of Solid State Chemistry

journal homepage: www.elsevier.com/locate/jssc

In-situ X-ray diffraction study of carbonate formation and decomposition in perovskite-type BCFZ

Konstantin Efimov*, Oliver Czuprat, Armin Feldhoff

Institute of Physical Chemistry and Electrochemistry, Leibniz Universität Hannover, Callinstr. 3A, D-30167 Hannover, Germany

ARTICLE INFO

Article history:
Received 19 October 2010
Received in revised form
7 March 2011
Accepted 10 March 2011
Available online 17 March 2011

Keywords:
Perovskite
BCFZ
CO_2 stability
Carbonate
Phase transition
In-situ XRD
TEM

ABSTRACT

The effect of CO_2 on the two phase perovskite with average composition of $BaCo_{0.4}Fe_{0.4}Zr_{0.2}O_{3-\delta}$ is investigated by *in-situ* X-ray diffraction (XRD) as well as transmission electron microscopy (TEM). Partial decomposition of the BCFZ into high-temperature rhombohedral $BaCO_3$ polymorph was observed during annealing in an atmosphere, which contained 50 vol% CO_2/50 vol% N_2 at 1173 K. This carbonate structure is not quenchable and cannot be detected by *ex-situ* methods. Additionally, the reversible phase transition of $BaCO_3$ from orthorhombic to rhombohedral to cubic at different temperatures accompanied by formation of CoO was shown by *in-situ* XRD and TEM. Furthermore, complete regeneration of perovskite phase was obtained after high-temperature treatment under CO_2-free conditions.

1. Introduction

Doped perovskites (ABO_3) with multivalent cations as mixed ionic and electronic conductors are a hot topic in materials science today, e.g. as membrane materials for the separation of oxygen from oxygen containing gases like air with unrivaled selectivities [1] or as cathode material in solid-oxide fuel cells [2]. In the last decade, these membranes have attracted great academic and industrial interest, since they have also large potential applications in chemical processes in which a constant supply or removal of oxygen is required [3]. For prospective industrial applications as membrane reactors for oxidative activation reactions of light hydrocarbons [4] or as oxygen separators in zero emission plants in which oxygen permeable membranes are flushed with CO_2-containing exhaust gases [5], a sufficient stability especially in reducing gas atmospheres or atmospheres containing CO_2 is essential.

The poisoning effect of CO_2 arises from alkaline earth metal cations in the perovskite structure, which tend to form carbonates. Carolan et al. [6] reported that the oxygen permeation flux of $La_{0.8}Ba_{0.2}Co_{0.8}Fe_{0.2}O_{3-\delta}$ decreased significantly when 430 ppm CO_2 was introduced into the operation gas. It was further discovered that $BaCe_{0.9}Y_{0.1}O_{3-\delta}$ is converted to the carbonate at 1123–1273 K under pure CO_2 atmosphere and the perovskite structure is disrupted [7].

Arnold et al. [8] investigated the influence of CO_2 on the oxygen permeation performance and the microstructure of perovskite-type $Ba_{0.5}Sr_{0.5}Co_{0.8}Fe_{0.2}O_{3-\delta}$ membranes. It was found that when having air on the feed side, using pure CO_2 as sweep gas at 1148 K caused an immediate stop of the oxygen permeation flux, which could be recovered by sweeping with pure helium. A detailed surface analysis of a BSCF cathode after operation in 1% CO_2/O_2 at 723 K for 24 h revealed that its surface was destroyed and mixed barium–strontium carbonate was formed as a top layer [9].

Systems using dense perovskite hollow fiber membranes of the composition $BaCo_xFe_yZr_zO_{3-\delta}$ ($x+y+z=1$), which is a novel oxygen permeable membrane material with high O_2 permeation fluxes and excellent thermal and mechanical stability [10], have been presented by our group, e.g. for the direct decomposition of nitrous oxide to nitrogen by *in-situ* oxygen removal [11], the simultaneous production of hydrogen and synthesis gas by combining water splitting with partial oxidation of methane [12] as well as the multi-step oxidative dehydrogenation of ethane [4] and propane (ODP) [13]. Furthermore, the oxidative coupling of methane to C_2 products could be successfully demonstrated in a $BaCo_xFe_yZr_zO_{3-\delta}$ hollow fiber membrane reactor [14].

Summarizing, the effect of CO_2 on the membrane permeation performance plays an important role and thus was examined recently [15]. Under exposure of 50 vol% CO_2 in He, the perovskite structure is impaired up to a depth of ca. 15 μm after 5 h and approximately 30 μm after 10 h, respectively. Furthermore, it was found that both microstructure as well as oxygen permeation are recovered in a CO_2-free atmosphere.

* Corresponding author.
E-mail address: Konstantin.Efimov@pci.uni-hannover.de (K. Efimov).

0022-4596/$ - see front matter © 2011 Elsevier Inc. All rights reserved.
doi:10.1016/j.jssc.2011.03.023

In order to get a deeper understanding of the processes occurring during application in CO_2 containing atmospheres, we carried out an *in-situ* X-ray diffraction (XRD) as well as transmission electron microscopy (TEM) study on the powder with the composition of $BaCo_{0.4}Fe_{0.4}Zr_{0.2}O_{3-\delta}$, which is similar to that of $BaCo_xFe_yZr_zO_{3-\delta}$ hollow fiber, and can be considered as a model system.

2. Experimental

Powder with average composition of $BaCo_{0.4}Fe_{0.4}Zr_{0.2}O_{3-\delta}$ (denoted as BCFZ) was obtained from the Fraunhofer-Institute for Ceramic Technologies and Systems (IKTS, Hermsdorf) from the hydrolysis of corresponding metal nitrates by an ammonium hydroxide solution followed by calcination. $BaCo_xFe_yZr_zO_{3-\delta}$ ($x+y+z=1$) hollow fiber membranes were manufactured by phase inversion spinning followed by sintering as described elsewhere [1]. The O_2 permeation experiments of the $BaCo_xFe_yZr_zO_{3-\delta}$ hollow fiber membrane, were carried out on a high-temperature permeation reactor which is described in detail elsewhere [1]. *In-situ* powder XRD was conducted on the Bruker D8 Advance diffractometer in Bragg-Brentano geometry using Cu-$K\alpha$ radiation with interval of 0.02 and count times of 0.3 s per step. The diffractometer was equipped with an Anton Paar 1200 N high-temperature chamber and superfast 1D Lynxeye detector. XRD data were analyzed using TOPAS 4.0 software (Bruker AXS). Quantitative analyses of XRD collected at isothermal conditions were carried out by Rietveld method. During the *in-situ* experiments at rising and falling temperatures, phases with unknown structures were observed. These phases were included in the refinement by Pawley fits. Then, the phase contents were estimated from the integrated scattered intensities of corresponding phases. The reliability of the both methods was controlled by XRD experiments on BCFZ powder at room temperature in ambient air using of known amount of $BaCO_3$ as internal standard. Structural data for the known phases were taken from ICSD database (FIZ Karlsruhe) with file numbers: $BaCoO_{2.23}$ [28865], $BaZrO_3$ [27048], $BaCO_3$ (orthorhombic) [15196], $BaCO_3$ (rhombohedral) [158389], $BaCO_3$ (cubic) [27449], CoO [28505], and FeO [24635]. Scanning TEM (STEM) was conducted at 200 kV on a JEOL JEM-2100 F-UHR field-emission instrument. A light-element energy dispersive X-ray (EDX) spectrometer, Oxford Instruments INCA-200 TEM, was used for elemental analysis. In order to obtain a TEM sample, the powder was glued between two alumina bodies, polished, and finally Ar^+ sputtered to electron transparency.

3. Results and discussion

The effect of CO_2 on the oxygen permeation performance of the $BaCo_xFe_yZr_zO_{3-\delta}$ hollow fiber at 1173 K is shown in Fig. 1. Insertion of 10 vol% CO_2 on the sweep side of a membrane leads to the diminution of oxygen permeation flux after only few minutes. Then, the oxygen flux through perovskite hollow fiber is almost stopped after dwell time of 30 min. However, the fast recovery of the oxygen permeation can be observed, if the sweep gas is changed to pure He. The value of oxygen flux reaches two-thirds of the initial performance after 5 min. The complete regeneration occurs after testing for 30 min.

According to Czuprat et al. [15], the decline of oxygen permeation flux in presence of CO_2 is due to formation of $BaCO_3$, which was observed by XRD and scanning electron microscopy (SEM) on the surface of quenched $BaCo_xFe_yZr_zO_{3-\delta}$ perovskite hollow fiber. The full recovery of the flux points out to the decomposition of poisoning $BaCO_3$ and the regeneration of the initial structure of hollow fiber.

To prove this hypothesis, the high-temperature *in-situ* XRD in CO_2 containing atmosphere was carried out on the BCFZ powder. Fig. 2 shows *in-situ* XRD-patterns of BCFZ collected at (a) room temperature, (b) at 1173 K in flowing synthetic air consisting 80 vol% N_2 and 20 vol% O_2, and (c) at 1173 K in an atmosphere

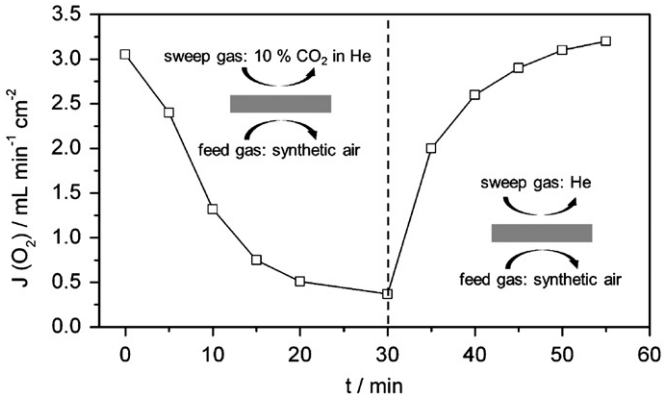

Fig. 1. Decline of O_2 permeation through a $BaCo_xFe_yZr_zO_{3-\delta}$ hollow fiber membrane with effective thickness of 140 μm under CO_2 exposure on the sweep side (sweep side: F_{total}=50 mL min^{-1} 10 vol% CO_2 in He; feed side: 150 mL min^{-1} synthetic air (80 vol% N_2, 20 vol% O_2,) and recovery as a function of time while sweeping with pure He at 1173 K (sweep side: 50 mL min^{-1} He; feed site: 150 mL min^{-1} synthetic air (80 vol% N_2, 20 vol% O_2,)).

containing 50 vol% CO_2 and 50 vol% N_2. As can be seen in the room temperature XRD (Fig. 2a), the original BCFZ powder consists of two perovskite systems as reported by Caro et al. [16] previously. The Rietveld analysis of XRD data combined with the EDXS investigation of the initial BCFZ powder exhibit, that the main compound is a $BaCo_{0.5-\gamma}Fe_{0.5-\gamma}Zr_{2\gamma}O_{3-\delta}$ (γ=0.015–0.025) with cubic structure (space group $Pm\bar{3}m$, a=4.072 Å). Furthermore, the powder contains approximately 16 wt% of cubic $BaZrO_3$ perovskite (space group $Pm\bar{3}m$, a=4.18 Å). Note, the co-existence of two cubic perovskite phases after doping of 5–10% Zr was also reported for similar perovskite systems like $Ba_{0.5}Sr_{0.5}Co_{0.8}Fe_{0.2-x}Zr_xO_{3-\delta}$ and $SrCo_{0.4}Fe_{0.6-x}Zr_xO_{3-\delta}$ [17,18]. The high-temperature XRD pattern taken from the BCFZ powder annealed at 1173 K for 30 min in the flowing synthetic air evidences no structural changes. Only slight shift of Bragg-reflection positions to smaller angles can be recognized here due to thermal lattice expansion. The annealing of the BCFZ powder at 1173 K for 90 min under 50 vol% CO_2/50 vol% N_2 leads to the partial decomposition of perovskite structure. $BaCO_3$ can be detected in the *in-situ* XRD pattern (Fig. 2c) alongside of BCFZ. The pattern of $BaCO_3$ relates to the high-temperature rhombohedral polymorph (space group $R3m$), which is stable in the temperature range from approximately 1073 K to 1233 K as reported by Antao et al. [19]. The structure of this phase is not quenchable and cannot be detected by *ex-situ* methods. Quantitative Rietveld analysis was applied to estimate the $BaCO_3$ content in the sample to be about 29 wt%. Additionally, the presence of a fourth phase is obvious by weak intensities at 36.3° and 42.1° 2Θ. This phase can be understood as CoO with help of TEM experiments (see Fig. 5) on the sample quenched in CO_2-containing atmosphere. Change-over of the gas atmosphere to the CO_2-free synthetic air or pure N_2 leads to the complete decomposition of $BaCO_3$ and regeneration of both perovskite phases.

In order to elucidate the kinetics of the carbonate formation and decomposition, series of *in-situ* XRD experiments accompanied by quantitative analysis were carried out determining the content of $BaCO_3$ in the BCFZ powder as function of time. Fig. 3 summarizes the results of quantitative analysis of diffraction patterns collected at 1173 K in time intervals of 15 min at different gas atmospheres. In presence of 50 vol% CO_2 in N_2, the content of $BaCO_3$ amounts to approximately 15 wt% after the first 15 min. After half an hour, the content of $BaCO_3$ reaches about 24 wt%. Then, the amount of carbonate increases slowly and reaches the value of approximately 29 wt% during 90 min. The sluggish kinetic of carbonate formation after the dwell time of 30 min may be explained by the development of the dense

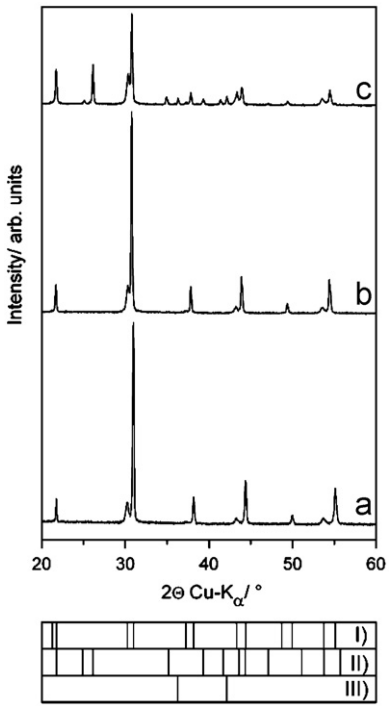

Fig. 2. *In-situ* XRD-patterns of BCFZ powder collected (a) at room temperature; (b) at 1173 K in flowing synthetic air (80 vol% N_2, 20 vol% O_2) after 30 min, $F_{total}=100$ mL min^{-1}; (c) at 1173 K in an atmosphere containing 50% CO_2/50% N_2 after 90 min, $F_{total}=100$ mL min^{-1}. (I–III) Calculated Bragg position of (I) BCFZ (two phase system); (II) $BaCO_3$ rhombohedral polymorph; (III) CoO.

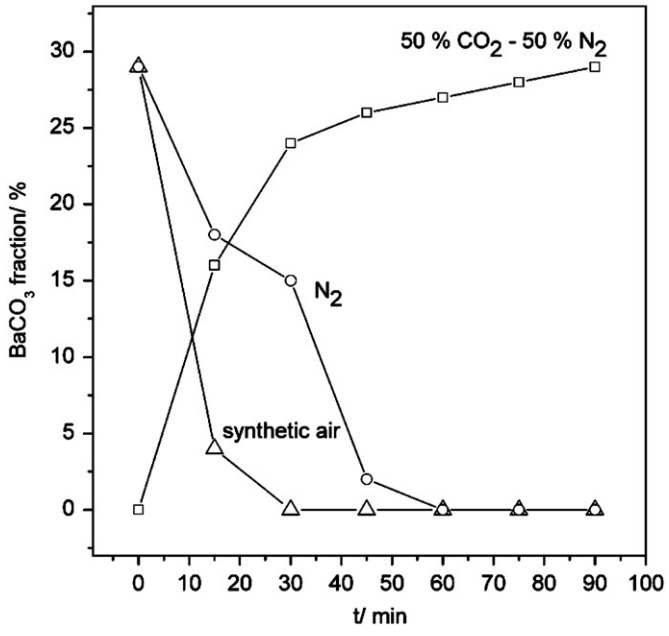

Fig. 3. Amount of $BaCO_3$ in the BCFZ sample as function of time at different atmospheres as observed by *in-situ* XRD. (Synthetic air: 80 vol% N_2, 20 vol% O_2, $F_{total}=100$ mL min^{-1}; N_2: $F_{total}=100$ mL min^{-1}).

carbonate layer on the surface of perovskite particles, which can be considered as a protective layer regarding further carbonate formation. Moreover, thermodynamical considerations deliver further approach to understand partial BCFZ decomposition. According to the Ellingham diagram presented by Feldhoff et al. [20], $BaCO_3$ is stable at 5×10^4 Pa CO_2 up to 1603 K. However, Kumar et al. [21] reported that the reaction of $BaCO_3$ with transition metal oxide like TiO_2 leading to the formation of perovskite is thermodynamically possibly above 649 K in 10^5 Pa CO_2. Thus, we assume that the reaction of the carbonate with transition metal oxide counteracts the formation of the carbonate at 1173 K in 5×10^4 Pa CO_2 and the both processes are in equilibrium state. The composition of remaining BCFZ perovskite, which consists of the two above mentioned perovskite phases was also changed during the annealing in CO_2. We found that the ratio of $BaCo_{0.5-\gamma}Fe_{0.5-\gamma}Zr_{2\gamma}O_{3-\delta}$ component was significantly decreased and reached the value of approximately 46 wt%. In contrast, the ratio of $BaZrO_3$ phase was remained almost constant. It seems that carbonate formation occurs at the costs of Co- and Fe-containing perovskite phase. These phenomena points out to the higher stability of Zr-based perovskite as postulated by Yokokawa et al. [22].

Fig. 3 shows also the kinetics of the BCFZ regeneration, if the CO_2 atmosphere was changed over to synthetic air or pure N_2. In air, the carbonate was decomposed very rapidly. After 15 min, only approximately 4 wt% carbonate can be detected in the sample. After 30 min, the carbonate was removed completely. Carbonate decomposition proceeds in the N_2 atmosphere a little slower. The perovskite structure was fully recovered after testing for 60 min. The decomposition of $BaCO_3$ in CO_2-free atmospheres corresponds to thermodynamical calculations, which indicate that carbonate becomes unstable at 1173 K if CO_2 partial pressure is lower than 30 Pa [20]. Then, solid state reaction between carbonate and transition metal oxides can be considered as thermodynamically favored.

Effect of temperature on the carbonate formation in the atmosphere containing 50 vol% CO_2 in N_2 was also studied by *in-situ* XRD during heating and cooling in the range of 303–1273 K with steps of 100 K. Before each data acquisition, an equilibrium time of 30 min was set. The phase fractions were estimated by considering integrated intensities of corresponding phases in the refinements, which were carried out by combined Rietveld and Pawley methods. Fig. 4a and b display selected XRD data. An appreciable amount of $BaCO_3$ was detected not until 873 K by heating of the sample (Fig. 4a). A low temperature orthorhombic polymorph (space group *Pmcn*) was formed under these conditions. Additionally, a low amount of CoO can be observed in the powder. The carbonate remains in orthorhombic symmetry up to 973 K. Rising the temperature leads to the phase transition of the orthorhombic $BaCO_3$ to rhombohedral polymorph at 1073 K and to cubic carbonate phase at 1273 K. The high-temperature cubic carbonate (space group $Fm\bar{3}m$) exists only at temperatures above 1233 K as reported by Strømme [23]. Interestingly, the integrated intensity of carbonate phase in the scan collected at 1073 K was diminished from 42% at 1073 K to 10% at 1273 K, which can be explained by strong decline of the carbonate content in the sample. This finding can be related to an increasing of the Gibbs free enthalpy of carbonate formation with rising temperature accompanied by decline of the Gibbs free enthalpy of the reaction between carbonate and oxides leading to shift of equilibrium of the processes [21]. During cooling, $BaCO_3$ structure changes to rhombohedral polymorph at 1173 K (Fig. 4b) and the integrated intensity of carbonate phase reaches the value of about 21%. Further cooling to 873 K leads to formation of orthorhombic carbonate phase and rising of the ratio of the integrated intensity to 27%.

Thus, the maximum $BaCO_3$ content in the sample was observed in the sample at 1073 K during the heating. Furthermore, the XRD scan collected at these conditions exhibits apparently just one perovskite phase. However, the value of scattered intensity of this phase amounted to be 52%, which cannot be explained by complete loss of Co- and Fe-containing phases. The shape of the peaks as well as peak widths cannot be interpreted by single $BaZrO_3$ phase also. Rather, the formation of above 40 wt% carbonate

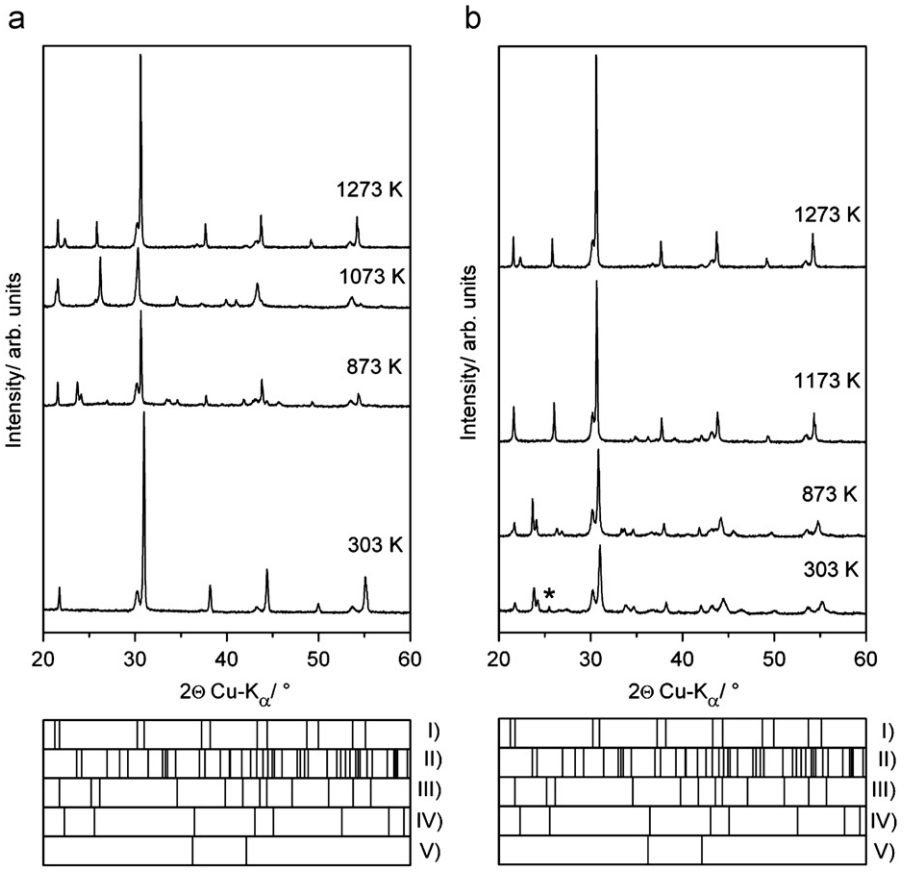

Fig. 4. *In-situ* XRD of BCFZ powder in the atmosphere containing 50 vol% CO_2 and 50 vol% N_2 $F_{total}=100$ mL min^{-1} (a) during heating; (b) during cooling. Before each data acquisition an equilibrium time of 30 min was set. (I–V) Calculated Bragg positions for (I) BCFZ; (II) orthorhombic $BaCO_3$; (III) rhombohedral $BaCO_3$; (IV) cubic $BaCO_3$; (V) CoO. Asterisks marks a reflection of tetragonal perovskite phase.

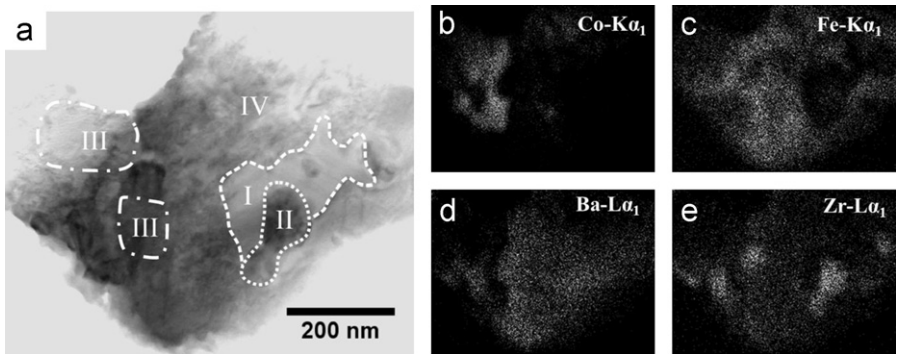

Fig. 5. (a) STEM bright field micrograph of BCFZ powder annealed and cooled in 50% CO_2 and 50% N_2. (b–e) Elemental distributions by EDXS.

leads to strong decline of Co- and Fe-ratio in the main perovskite phase followed by increase of lattice parameter due to high amount of Zr in the perovskite. Consequently, the increase of lattice parameter leads to a shift of the reflection positions to the smaller 2Θ angles and to the overlap of the reflection positions of both perovskite phases in the corresponding XRD scan. Increase of the temperature to 1273 K leads to partial decomposition of $BaCO_3$ due to the above-mentioned reasons and to a regeneration of $BaCo_{0.5-\gamma}Fe_{0.5-\gamma}Zr_{2\gamma}O_{3-\delta}$ phase. The composition of the sample was marginally changed after the complete cooling in CO_2. However, at room temperature we detected a new compound in XRD pattern, which cannot be attributed to the mentioned phases. The intensity of the phase at 25.4° 2Θ, which is marked by asterisks in Fig. 4b, relates to a tetragonal perovskite structure as reported by Martynczuk et al. [24].

In order to verify the results of *in-situ* XRD experiments, we investigated the sample, which was annealed and cooled down in CO_2 by TEM methods. The STEM bright-field micrograph in Fig. 5a shows a BCFZ powder particle, which consists of several grains. EDXS elemental distribution (Fig. 5b–e) clearly demonstrates that the grains exhibit a different chemical composition. The grain marked in Fig. 5a with "I" contains no metal cations besides of Ba and can be indicated as $BaCO_3$. Obviously, the carbonate phase does not form a dense layer around the BCFZ powder particle in contrast to the hollow fiber ceramic membrane [15]. Instead, the carbonate is located inside of the particle. This kind of behavior was also observed by Martynczuk et al. [24], who investigated the effect of CO_2 on the functional performance of related Zn-doped $(Ba,Sr)FeO_{3-\delta}$ perovskite. The phase "II" consisted of Ba and Zr in the ratio 1:1 relates to $BaZrO_3$. Cliff-Lorimer quantification of EDXS

data reveals a dramatical enrichment of Co in area "III" collateral to an almost entirely absence of other cations. Thus, this phase can be considered as CoO. Finally, the main phase marked with "IV" can be described as a Co-depleted $Ba(Co,Fe,Zr)O_{3-\delta}$ perovskite.

Based on the *in-situ* XRD study as well as TEM investigations, we summarize the BCFZ decomposition process in presence of CO_2. Firstly, the CO_2 reacts with BCFZ under formation of $BaCO_3$. The carbonate can exhibit different polymorphs depending on the temperature. The formation of carbonate does not lead to the complete destruction of perovskite. Based on TEM, partial BCFZ decomposition cannot be explained by slow kinetic of the reaction due to formation of protective layer on the surface of perovskite particle. The chemical equilibrium between formation of carbonate and reaction to the perovskite can be rather considered as an applicable approach. Second, we found that the carbonate formation occurs predominantly at the cost of Co/Fe containing component of BCFZ accompaned by development of CoO as by-product. Poor stability of Co-containing perovskite caused by flexible redox behavior of Co-cations was already discussed in some details in ours previous reports [25–27]. Furthermore, these results are in good agreement with reports of Yakovlev et al. [17] as well as Yi et al. [28] suggesting the stabilizing effect of higher valent *B*-site cation like Zr^{4+} or Nb^{5+} on the Co-, Fe-containing perovskite materials. The remaining perovskite phase was found to be Fe-enriched. According to the report of Yáng et al. [29], structures of perovskites with Ba/Fe-rich composition exhibit several distorted variants. One of them, the tetragonal distorted perovskite phase, we observed in the room temperature XRD pattern (Fig. 4b).

4. Conclusions

Decomposition process of BCFZ powder, which consists of two perovskite phases, in the CO_2-containing atmosphere was investigated by *in-situ* XRD as function of dwell time and temperature. Rapid formation of high-temperature rhombohedral $BaCO_3$ polymorph was observed after exposure of the CO_2 at 1173 K. This non-quenchable carbonate structure, which is stable at temperatures between 1073 and 1233 K, can be declared as the phase terminating the oxygen permeation transport through BCFZ membrane materials. Time-dependent experiments at isothermal conditions deliver the partial decomposition of two phase BCFZ system at the costs of Co- and Fe-containing perovskite phase, which is in close agreement with thermodynamical considerations. Furthermore, the complete regeneration of BCFZ was proven after removing of CO_2 from the gas atmosphere.

The reversible phase transition of $BaCO_3$ from orthorhombic at temperatures below 1073 K to rhombohedral to cubic at 1273 K was shown by *in-situ* XRD. Finally, formation of CoO as well as traces of tetragonal disordered Fe-enriched perovskite phase was observed as by-products of BCFZ decomposition by XRD and TEM methods.

Acknowledgments

K.E. and A.F. gratefully acknowledge financial support by the State of Lower Saxony (Germany, NTH bottom-up project, No. 21-71023-25-7/09). O.C. appreciates funding from the European Union's Seventh Framework Program FP7/2007-2013 under grant agreement No. 228701. The authors gratefully acknowledge fruitful discussions with Prof. Jürgen Caro.

References

[1] T. Schiestel, M. Kilgus, S. Peter, K.J. Caspary, H. Wang, J. Caro, J. Membr. Sci. 258 (2005) 1–4.
[2] Z. Shao, S. Haile, Nature 431 (2004) 170–173.
[3] H.J.M. Bouwmeester, A.J. Burggraaf, Dense ceramic membranes for oxygen separation, in: A.J. Burggraaf, L. Cot (Eds.), Fundamentals of Inorganic Membrane Science and Technology, Elsevier, Amsterdam, 1996, pp. 435–528.
[4] O. Czuprat, S. Werth, S. Schirrmeister, T. Schiestel, J. Caro, Chem. Catal. Chem. 1 (2009) 401–405.
[5] J.H. Horlock, Advanced Gas Turbine Cycles, Pergamon, Oxford, 2003.
[6] M.F. Carolan, P.N. Dyer, J.M LaBar, R.M. Thorogood, US Patent 5240473 (1993).
[7] N. Zakowsky, S. Williamson, J.T.S. Irvine, Solid State Ionics 176 (2005) 3019–3026.
[8] M. Arnold, H. Wang, A. Feldhoff, J. Membr. Sci. 293 (2007) 44–52.
[9] A. Yan, V. Maragou, A. Arico, M. Cheng, P. Tsiakaras, Appl. Catal. B 76 (2007) 320–327.
[10] S.M. Liu, G.R. Gavalas, J. Membr. Sci. 246 (2005) 103–108.
[11] H. Jiang, H. Wang, F. Liang, S. Werth, T. Schiestel, J. Caro, Angew. Chem. Int. Ed. 48 (2009) 2983–2986.
[12] H. Jiang, H. Wang, S. Werth, T. Schiestel, J. Caro, Angew. Chem. Int. Ed. 47 (2008) 9341–9344.
[13] O. Czuprat, S. Werth, J. Caro, T. Schiestel, AIChE J. 56 (2010) 2390–2396.
[14] O. Czuprat, T. Schiestel, H. Voss, J. Caro, Ind. Eng. Chem. Res. 46 (2010) 10230–10236.
[15] O. Czuprat, M. Arnold, S. Schirrmeister, T. Schiestel, J. Caro, J. Membr. Sci. 364 (2010) 132–137.
[16] J. Caro, H. Wang, C. Tablet, A. Kleinert, A. Feldhoff, T. Schiestel, M. Kilgus, P. Kölsch, S. Werth, Catal. Today 118 (2006) 128–135.
[17] S. Yakovlev, C.Y. Yoo, S. Fang, H.J.M. Bouwmeester, Appl. Phys. Lett. 96 (2010) 254101-1.
[18] L. Yang, L. Tan, X. Gu, W. Jin, L. Zhang, N. Xu, Ind. Eng. Chem. Res. 42 (2003) 2299–2305.
[19] S.M. Antao, E.I. Hassan, Phys. Chem. Miner. 34 (2007) 573–580.
[20] A. Feldhoff, M. Arnold, J. Martynczuk, Th.M. Gesing, H. Wang, Solid State Sci. 10 (2008) 689–701.
[21] S. Kumar, G.L. Messing, W.B. White, J. Am. Ceram. Soc. 76 (1993) 617–624.
[22] H. Yokokawa, N. Sakai, T. Kawada, M. Dokiya, Solid State Ionics 52 (1992) 43–56.
[23] K.O. Strømme, Acta Chem. Scand. A 29 (1975) 105–110.
[24] J. Martynczuk, K. Efimov, L. Robben, A. Feldhoff, J. Membr. Sci. 344 (2009) 62–70.
[25] K. Efimov, T. Halfer, A. Kuhn, P. Heitjans, J. Caro, A. Feldhoff, Chem. Mater. 22 (2010) 1540–1544.
[26] A. Feldhoff, J. Martynczuk, M. Arnold, M. Myndyk, I. Bergmann, V. Šepelák, W. Gruner, U. Vogt, A. Hähnel, J. Woltersdorf, J. Solid State Chem. 182 (2009) 2961–2971.
[27] K. Efimov, Q. Xu, A. Feldhoff, Chem. Mater. 22 (2010) 5866–5875.
[28] J. Yi, M. Schroeder, T. Weirich, J. Mayer, Chem. Mater. 22 (2010) 6246–6253.
[29] Z. Yáng, A.S. Harvey, A. Infortuna, L. Gauckler, J. Appl. Crystallogr. 42 (2009) 153–160.